Available online at www.sciencedirect.com

ScienceDirect

Proceedings of the Combustion Institute 38 (2021) 5905–5913

Proceedings of the Combustion Institute

www.elsevier.com/locate/proci

Autoignition and detonation development from a hot spot inside a closed chamber: Effects of end wall reflection

Peng Dai [a,*], Zheng Chen [b], Xiaohua Gan [a], Mikhail A. Liberman [c]

[a] *Department of Mechanics and Aerospace Engineering, Southern University of Science and Technology, Shenzhen 518055, China*

[b] *SKLTCS, CAPT, BIC-ESAT, College of Engineering, Peking University, Beijing 100871, China*

[c] *Nordita, KTH Royal Institute of Technology and Stockholm University, Roslagstullsbacken 23, SE-10691 Stockholm, Sweden*

Received 20 October 2019; accepted 10 September 2020
Available online 13 October 2020

Abstract

The advancement of highly boosted internal combustion engines (ICEs) with high thermal efficiency is mainly constrained by knock and super-knock, respectively, due to the end gas autoignition and detonation development. The pressure wave propagation and reflection in a small confined space may strongly interact with local end gas autoignition, leading to combustion characteristics different from those in a large chamber or open space. The present study investigates the transient autoignition process in an iso-octane/air mixture inside a closed chamber under engine-relevant conditions. The emphasis is given to the assessment of effects of the pressure wave-wall reflection and the mechanism of extremely strong pressure oscillation typical for super-knock. It is found that the hot spot induced autoignition in a closed chamber can be greatly affected by shock/pressure wave reflection from the end wall. Different autoignition modes respectively from the hot spot and the end wall reflection are identified. A non-dimensional parameter quantifying the interplay between different length and time scales is introduced, which helps to identify different autoignition regimes including detonation development near the end wall. It is shown that detonation development from the hot spot may cause super-knock with devastating pressure oscillation. However, the detonation development from the end wall can hardly produce pressure oscillation strong enough for the super-knock. The obtained results provide a fundamental insight into the knocking mechanism in engines under highly boosted conditions.

Keywords: Autoignition; Detonation development; End wall reflection; Pressure oscillation; Iso-octane

1. Introduction

Downsized and turbocharged spark ignition engines (SIEs) have attracted increasing interest due to their advantages of higher thermal efficiency and

* Corresponding author.
E-mail address: daip@sustech.edu.cn (P. Dai).

https://doi.org/10.1016/j.proci.2020.09.025
1540-7489

lower fuel consumption. However, the tendency of knock and super-knock is greatly enhanced in highly boosted environment [1,2], which remains a major limitation for the development of modern internal combustion engines (ICEs). Unlike conventional knock, super-knock is characterized by extremely high and destructive pressure oscillations (usually above 20 MPa) and it occurs stochastically in highly boosted SIEs [1,3,4]. While conventional knock has direct relevance to end gas autoignition, super-knock is found to be closely associated with detonation development induced by randomly localized hot spot [3–5]. Besides, lubricant oil droplets [6], particles [7] and deposits [8] can also be possible sources of super-knock. However, the detailed mechanism of super-knock with destructive in-cylinder pressure oscillation is still not well understood. Usually knock and super-knock occur inside a small confined space towards the end of the power stroke. In a closed and relatively small chamber, propagation and reflection of pressure waves from the chamber walls may strongly interact with local end gas autoignition, leading to combustion characteristics different from those in a large chamber or open space. Therefore, understanding of autoignition and detonation development in a confined space under engine-relevant conditions is of fundamental interest.

A number of studies have been conducted to understand autoignition induced by thermal and/or composition non-uniformity in reactive mixtures. Zel'dovich et al. [9,10] first analyzed different modes of autoignition front propagation caused by reactivity gradient. Bradley and co-workers [11,12] further investigated autoignition induced by a hot spot and identified a detonation peninsula in the plot of two non-dimensional parameters: the normalized temperature gradient (ξ) and the ratio of acoustic time to excitation time (ε). This detonation peninsula was widely utilized in the studies on knock and super-knock [3,13–16]. Besides, Liberman and co-workers [17,18] studied the combustion regimes induced by initial temperature gradient. They found that the temperature gradient initiating a detonation predicted by detailed chemical models greatly differs from that predicted using a one-step chemistry. Sow et al. [19] analyzed the effects of thermal stratification in bulk end gas on detonation development. In our recent publications [20–25], autoignition and detonation development of large hydrocarbon fuels with negative temperature coefficient (NTC) were investigated. It was found that the low-temperature chemistry greatly complicates the interaction between chemical reaction and pressure wave and that both temperature gradient (i.e. hot spot or cold spot) and concentration gradient can induce detonation development under proper conditions.

Previous studies have been focused mainly on the effects of local reactivity non-uniformity and bulk mixture properties on end gas autoignition

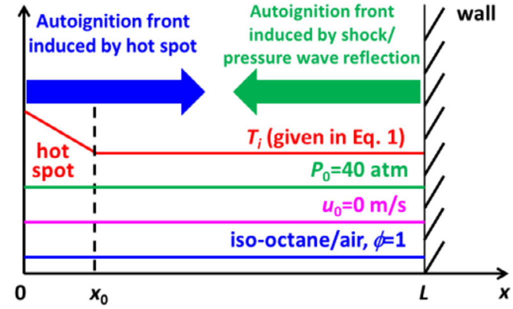

Fig. 1. Schematic of autoignition initiated by a hot spot in iso-octane/air mixture inside a closed chamber.

and detonation development. However, only a few studies considered the influence of pressure wave propagation and reflection inside a small confined space. Yu et al. [26,27], Pan et al. [28,29] and Terashima et al. [30,31] investigated the interaction between normal flame propagation, end gas autoignition and pressure wave in a closed chamber. However, the effects of wall reflection on autoignition and detonation development from local reactivity non-uniformity have not been systematically investigated. The objectives of this study are three-fold: (1) to investigate the transient autoignition process induced by a hot spot inside a small closed chamber, (2) to quantitatively describe the corresponding autoignition modes by using different non-dimensional parameters, and (3) to assess and interpret the effects of wall reflection and investigate the mechanism of extremely strong pressure oscillation typical for super-knock.

2. Numerical model

As the main component of the primary reference fuel (PRF) for gasoline, iso-octane is considered in this study. The reduced PRF mechanism [32] is used in simulations. Its performance in terms of predicting autoignition and flame propagation is demonstrated in the Supplemental Material and Ref. [32].

We consider the 1D transient autoignition process in the stoichiometric iso-octane/air mixture initiated by a hot spot in an adiabatic, closed chamber. In the present study turbulence is not considered. The initial conditions are shown in Fig. 1. The initial hot spot is characterized by the linear temperature distribution:

$$T_i(x) = \begin{cases} T_{i,0} + (x - x_0)(dT/dx)_i & \text{for } 0 \le x \le x_0 \\ T_{i,0} & \text{for } x_0 < x \le L \end{cases} \quad (1)$$

where x is spatial coordinate; x_0 is the hot spot size and L is the chamber length; $(dT/dx)_i$ is the temperature gradient within the hot spot, and $T_{i,0} = 900$ K is the initial temperature outside the hot spot. It is noted that turbulence might greatly affect the autoignition process when the time scales of physical-chemical processes are comparable with the Kolmogorov turbulent turnover time, which is beyond the scope of the current work.

The transient autoignition process is simulated using the in-house code A-SURF [21,33] which solves the conservation equations for one-dimensional, adiabatic, multi-component, reactive flow using the finite volume method. A multi-level, dynamically adaptive mesh refinement algorithm is adopted to ensure adequate numerical resolution of the reaction zone, pressure/shock wave, and detonation, which are always covered by the finest mesh of 3.125 μm. The time step is 3.125×10^{-10} s. The total physical time considered in simulations is around 4 ms, which is long enough for clear demonstration of the pressure oscillation at the end wall. Details on the governing equations, numerical scheme, and grid convergence can be found in Refs. [20,21,24,33] and thereby are not repeated here.

3. Results and discussion

3.1. Typical autoignition cases

As shown in Fig. 1, there might be two types of autoignition happening in a small chamber: (1) a rightwards propagating autoignition front induced by the hot spot, and (2) a leftwards propagating autoignition front from the end wall induced by shock/pressure wave reflection.

The autoignition front propagation initiated by hot spot in large or open space has been extensively studied [11,12,17,20–25]. According to the theory of Zel'dovich [10], there is a critical temperature gradient at which the autoignition front propagation speed, u_a, is equal to the sound speed, a; and it is defined as [11,12]:

$$(dT/dx)_c = (a(d\tau/dT_0))^{-1} \tag{2}$$

where τ is the ignition delay time (defined as the time for maximum heat release rate). The values of τ, $(dT/dx)_c$ and excitation time (τ_e, defined as the time interval between 5% and maximum heat release rate [11]) are shown in Fig. S2 in the Supplemental Material. The normalized temperature gradient of the hot spot, ξ, is defined as [11,12]:

$$\xi = (dT/dx)_i/(dT/dx)_{c,x_0/2} \tag{3}$$

where the subscript $x_0/2$ denotes that the value of critical temperature gradient is evaluated at $x = x_0/2$ in order to represent the average condition within the hot spot. The theoretical autoignition front propagation speed, u_a, can thereby be expressed as [11,12]:

$$u_a = a/\xi \tag{4}$$

The transient autoignition process at different hot spot sizes (x_0), temperature gradients (ξ) and chamber lengths (L) is systematically investigated. Nine typical cases are discussed below with the corresponding details summarized in Table S1 in the Supplemental Material.

Figure 2 shows the autoignition processes for three typical cases: case 1 (ξ=5.4, x_0=5 mm, L = 2 cm) for reference, case 2 (ξ=5.4, x_0=5 mm and L = 1 cm) with shorter chamber length, and case 3 (ξ=9.3, x_0=5 mm and L = 2 cm) with larger ξ. S denotes the transient propagation speed of the autoignition front. For autoignition initiated by the hot spot, three modes occur sequentially with the increase of ξ [22]: (I) supersonic reaction front propagation, (II) detonation development, and (III) subsonic reaction front propagation. For cases 1 and 2 shown in Fig. 2(a) and (b), a detonation wave develops inside the hot spot and thereby they correspond to autoignition mode II. The detonation development is caused by strong coherent coupling and mutual amplification between chemical reaction and pressure wave. On the other hand, Fig. 2(c) shows that for higher value of ξ, a leading shock wave is generated ahead of the autoignition front, which is the result of weaker chemical-acoustic interaction at reduced autoignition front propagation speed (see Eq. (4)) [20,21]. The autoignition front behind the shock wave gradually develops to a detonation wave due to the compression and heating of upstream mixture by the shock wave. This autoignition mode was also observed in Ref. [20,21] and it is referred as mode IIs ("s" denotes "shock wave") in this study.

On the other hand, line #6 in Fig. 2(a) indicates that autoignition occurs near the end wall before the arrival of the detonation wave and that it produces a supersonic autoignition front propagating to the left. This autoignition mode near the end wall is thereby referred as W.A. (Wall Autoignition). The rightwards propagating detonation wave quenches after encountering the leftwards propagating autoignition front since all the reactants are consumed; and it degenerates to a shock wave propagating to the right (see lines #7–9 in Fig. 2a).

When the chamber length is reduced as in case 2, no autoignition near the end wall is observed. This is mainly because the time for the detonation wave propagation is shorter than the autoignition time near the end wall. This mode near the wall is hence referred as W.N. (Wall with Non-autoignition). The mode W.N. is also observed in case 3 with larger ξ. Therefore, for both cases 2 and 3, the detonation wave can reach the end wall and their shock wave reflection is much stronger than that in case 1. This is demonstrated in Fig. 3, which shows the temporal evolution of pressure at the end wall for cases 1, 2 and 3.

The pressure oscillation in Fig. 3 is caused by the back-and-forth propagation of detonation/shock/pressure waves in the closed chamber.

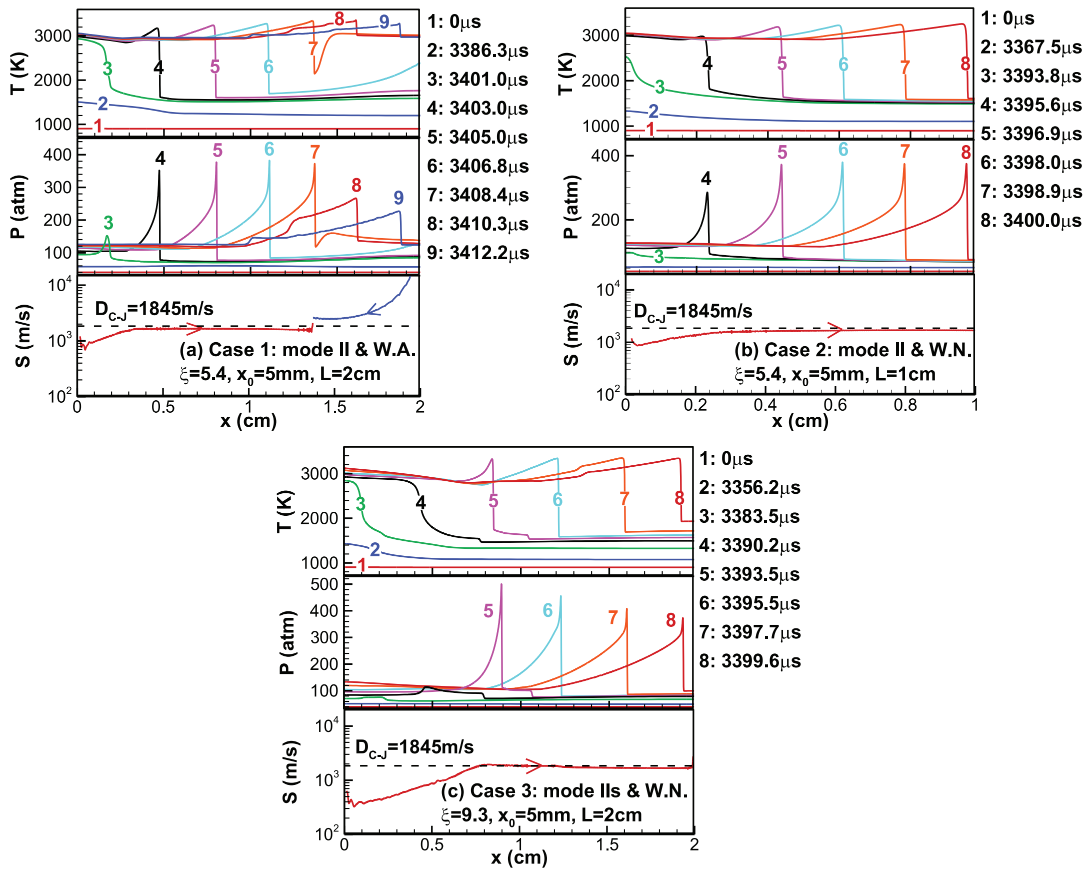

Fig. 2. Temporal evolution of temperature and pressure profiles and transient autoignition front propagation speed, S, for (a) case 1, (b) case 2, and (c) case 3. The arrows in the bottom sub-figures denote the propagation direction of autoignition fronts. The horizontal dashed lines indicate the C-J detonation wave speed, $D_{C\text{-}J}$.

It is seen that the maximum pressure oscillation amplitudes in cases 2 and 3 are much higher than that in case 1. As shown in Fig. 2, this is because the detonation waves in cases 2 and 3 directly hit against the end wall and generate extremely high pressure via reflection, while the detonation wave in case 1 degenerates to a shock wave before reaching the end wall. Therefore, a combination of mode II or IIs from the hot spot and mode W.N. near the end wall results in the strongest pressure oscillation and most severe damage to the engine cylinder. The extremely high pressure oscillation amplitudes in cases 1, 2 and 3 are, respectively, around 270 atm, 1130 atm, and 780 atm, which may all correspond to the super-knock phenomenon in SIEs. It is noted that the pressure oscillation amplitudes presented in this study are obtained through 1D simulations, and thereby cannot be directly compared with those in SIEs.

Figure 4 shows the autoignition processes in case 4 (ξ=12.9, x_0=5 mm and L=2 cm) and case 5 (ξ=14.6, x_0=5 mm and L=2 cm) with further increase in the value of ξ. It is observed that the autoignition mode from the hot spot transits to subsonic reaction front propagation with a leading shock wave, which is referred as mode IIIs ("s" denotes "shock wave"). On the other hand, the mixture near the end wall autoignites in both cases 4 and 5 due to compression by the reflected shock wave. However, while a leftwards propagating supersonic autoignition front is generated in case 4 (i.e. mode W.A.), a detonation wave is formed from the end wall in case 5, which is referred as mode W.D. (Wall Detonation). The detonation wave quenches when it encounters the rightwards propagating autoignition wave and degenerates to a shock wave that propagates to the left in the burnt mixture (see lines #9 and #10 in Fig. 4b).

Figure 5 shows the temporal evolution of pressure at the end wall in cases 4 and 5. It is observed that although a detonation wave is formed from the end wall in case 5, the corresponding pressure oscillation amplitude is very close to that in case 4 without detonation development, which are both

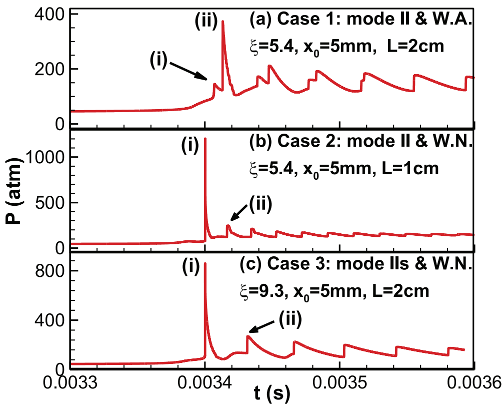

Fig. 3. Temporal evolution of pressure at the end wall for (a) case 1, (b) case 2, and (c) case 3. The marked pressure peaks correspond to: (i) autoignition near the end wall, (ii) reflection of shock wave remaining from the quenching detonation wave in Sub-figure (a); and (i) reflection of detonation wave, (ii) reflection of shock wave remaining from the quenching reflected detonation wave in Sub-figures (b) and (c).

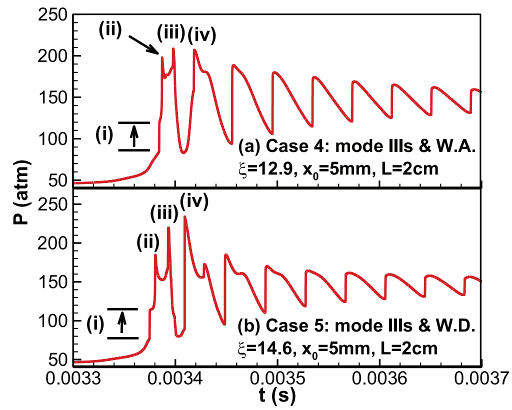

Fig. 5. Temporal evolution of pressure at the end wall for (a) case 4 and (b) case 5. The marked pressure peaks correspond to: (i) reflection of leading shock wave, (ii) autoignition near the end wall, (iii) reflection of pressure wave formed by the autoignition front from the hot spot, and (iv) reflection of shock waves respectively (a) formed by the supersonic autoignition front from the end wall and (b) remaining from the quenching detonation wave from the end wall.

much lower than those in cases 1–3 with detonation wave initiated from the hot spot. This is because the leftwards propagating shock wave remaining from the quenching detonation wave in case 5 has to propagate forward and back through the chamber before arriving at the end wall, which significantly weakens its strength. Therefore, the detonation wave generated from the end wall (i.e. mode W.D.) may not cause damage as severe as the detonation wave from the hot spot (i.e. modes II and IIs)

The autoignition process in case 6 (ξ=16.2, x_0=5 mm and L = 2 cm) with further increased ξ is shown in the Supplemental Material. It is noted that the corresponding autoignition mode is essentially the same as that in case 4 (i.e. mode IIIs & W.A.) and a detonation wave is not developed. Besides cases 1–6 with x_0=5 mm, we also consider cases with smaller hot spot of x_0=3.5 mm, including case 7 (ξ=5.4, L = 2 cm, mode II & W.A.), case 8 (ξ=9.5, L = 2 cm, mode IIs & .W.A.), and case 9 (ξ=14.8, L = 2 cm, mode IIIs & W.A.). The corresponding autoignition processes are presented in the Supplemental Material.

3.2. Map of various autoignition modes

The above results indicate that the autoignition in a small chamber is essentially a combination of

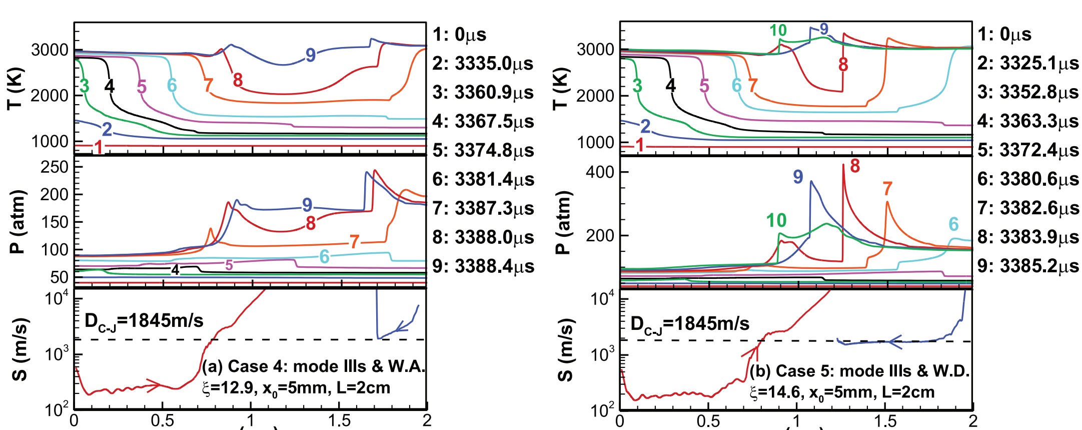

Fig. 4. Temporal evolution of temperature and pressure profiles and transient autoignition front propagation speed for (a) case 4 and (b) case 5.

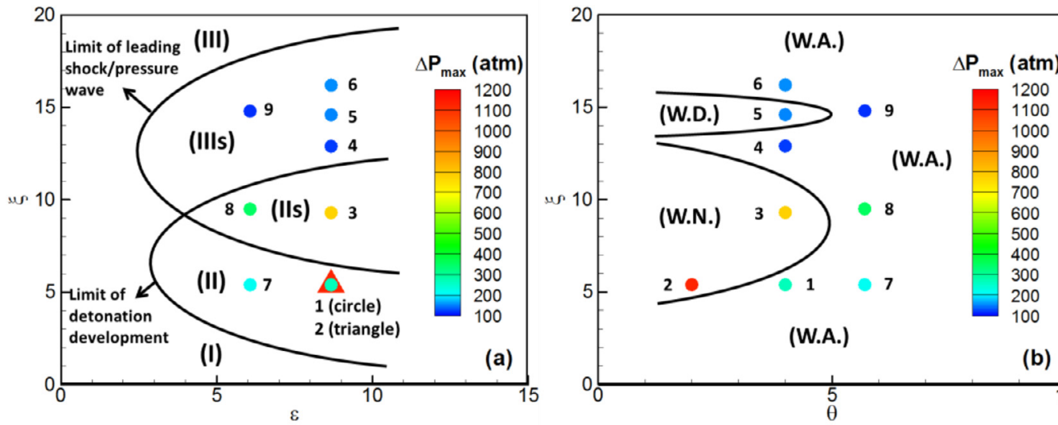

Fig. 6. Regimes of autoignition modes which are respectively (a) initiated by the hot spot and (b) induced by shock/pressure wave reflection on the end wall. Cases 1–9 are also plotted with the corresponding maximum pressure oscillation amplitude at the end wall, ΔP_{max}, indicated by the color scale.

the autoignition initiated by the hot spot and that induced by the shock/pressure wave reflection on the end wall.

For the autoignition from the hot spot, five modes are sequentially identified with the increase of ξ, namely: supersonic reaction front propagation (I), detonation development without leading shock wave (II), detonation development with leading shock wave (IIs), subsonic reaction front propagation with leading shock/pressure wave (IIIs), and subsonic reaction front propagation without leading shock/pressure wave (III). Figure 6(a) shows the corresponding regimes of these autoignition modes in ξ-ε diagram. The non-dimensional parameter, ε, is defined as the ratio of the acoustic time, x_0/a, to the excitation time, τ_e (i.e. $\varepsilon = x_0/(a\tau_e)$) [11]. It is noted that the strength of the leading shock/pressure wave in regime IIIs decreases with ξ. That is because the speed of the subsonic reaction front decreases with increasing ξ and thereby the coherent chemical-acoustic interaction is weakened. When ξ is sufficiently large, no shock/pressure wave is generated within the hot spot and the autoignition mode transits from mode IIIs to mode III.

On the other hand, three autoignition modes are identified near the end wall, which are respectively: autoignition with supersonic reaction front propagation (W.A.), non-autoignition (W.N.), and autoignition with detonation development (W.D.). There are four important factors affecting the autoignition mode near the end wall:

(1) The time elapsed between the autoignition in the hot spot and that at the end wall, which can be represented by the difference between 0D ignition delay at the hot spot ($x = 0$) and that at the end wall ($x = L$):

$$\Delta\tau_{0D} = \tau_{0D,\ wall} - \tau_{0D,\ hot\ spot} \tag{5}$$

According to Eqs. (1)–(3), we have

$$\begin{aligned}\Delta\tau_{0D} &= (d\tau/dT_0)\left(T_{i,wall} - T_{i,hot\ spot}\right)\\ &= (d\tau/dT_0)(dT/dx)_i x_0\\ &= (d\tau/dT_0)(\xi(dT/dx)_c)x_0 = \xi x_0/a\end{aligned} \tag{6}$$

(2) The autoignition front from the hot spot propagates to the end wall during time:

$$t_a = L/S \sim L/u_a = L\xi/a \tag{7}$$

(3) The leading shock/pressure wave from the hot spot propagates to the end wall during time:

$$t_{wave} \sim L/a \tag{8}$$

(4) The strength of the leading shock/pressure wave, I_{wave}, which is defined as the pressure increase across the shock/pressure wave.

It is convenient to introduce a non-dimensional parameter,

$$\theta = L/x_0 \tag{9}$$

to characterize the interplay between the length scales L and x_0 as well as that between the time scales t_a and $\Delta\tau_{0D}$. Substituting Eqs. (6) and (7) into (9) yields

$$\theta = (L\xi/a)/(\xi x_0/a) \sim t_a/\Delta\tau_{0D} \tag{10}$$

Figure 6(b) shows the autoignition regimes near the end wall in ξ-θ diagram. Note that the ξ-θ diagram might be affected by the fuel type and thermal conditions, which deserves further studies. The transition of autoignition modes with increasing ξ for cases 1, 3–6 is explained below.

(1) The transition from mode W.A. to W.N. and W.N. to W.A. for $\xi < 13$ is a result of competition between increasing $\Delta\tau_{0D}$ and t_a. When ξ is relatively small, the increase of ξ leads to

a longer $\Delta\tau_{0D}$ (see Eq. (6)) which dominates and delays the autoignition near the end wall relative to that in the hot spot. Therefore, the autoignition transits from mode W.A. in case 1 to mode W.N. in case 3. However, with further increase of ξ, the autoignition mode from the hot spot changes from detonation development to subsonic reaction front propagation with leading shock wave. Therefore, the mixture near the end wall gets compressed first by the reflected shock wave when t_a exceeds t_{wave}, and autoignition occurs before the arrival of the reaction front from the hot spot if t_a is sufficiently long. In other words, at relatively large ξ, the effect of increasing t_a with ξ dominates, which gives more time for autoignition of the mixture near the end wall due to the reflected shock wave. This leads to further transition from mode W.N. in case 3 to mode W.A. in case 4.

(2) The transition from mode W.A. to W.D. and W.D. to W.A. for $\xi > 13$ is a result of competition between increasing t_a and decreasing I_{wave}. At the beginning, an increase in ξ leads to further increase in t_a, so that the autoignition front initiated from the end wall has more time to form a detonation wave behind the reflected shock/pressure wave. Therefore, the autoignition mode transits from W.A. in case 4 to W.D. in case 5. However, when ξ further increases, the strength of leading shock/pressure wave, I_{wave}, decreases to the extent that the reflected shock/pressure wave from the wall can no longer initiate a detonation wave. Therefore, the autoignition mode transits from W.D. in case 5 to W.A. in case 6.

According to Eq. (10), lower value of θ implies less time needed for the autoignition front from the hot spot to propagate to the end wall (i.e. shorter t_a) or longer time for the mixture near the end wall to autoignite after the hot spot autoignition (i.e. longer $\Delta\tau_{0D}$), either of which reduces the tendency of autoignition near the end wall and is favorable to mode W.N. Therefore, the regime of mode W.N. expands with decreasing θ and lies within a reversed C-shaped curve in ξ-θ diagram.

As for mode W.D., according to Eqs. (6) and (8), the ratio between the time scales $\Delta\tau_{0D}$ and t_{wave} is:

$$\Delta\tau_{0D}/t_{wave} \sim (\xi x_0/a)/(L/a) = \xi/\theta \tag{11}$$

Higher value of $(\Delta\tau_{0D}/t_{wave})$ indicates that either the autoignition front initiated from the end wall has more time to form detonation wave before thermal explosion throughout the chamber (i.e. longer $\Delta\tau_{0D}$) or the mixture near the end wall is earlier compressed by the reflected shock/pressure wave (i.e. shorter t_{wave}). Therefore, increase of (ξ/θ) promotes detonation development from the end wall, which implies that the slope of the lower limit of W.D. regime is positive in ξ-θ diagram.

On the other hand, either smaller x_0 (i.e., larger θ, see Eq. (9)) or larger ξ around W.D. regime weakens the chemical-acoustic interaction within the hot spot and thereby leads to lower strength of leading shock/pressure wave, I_{wave}, which reduces the tendency of detonation development from the end wall. Therefore, the slope of the upper limit of W.D. regime is negative. Summarizing, W.D. regime lies within a reversed C-shaped curve in ξ-θ diagram.

Figure 6 provides a fundamental insight into the conditions for various autoignition modes induced by hot spot in a small chamber and those for super-knock in ICEs, which can be quantitatively described in ξ-ε and ξ-θ diagrams. It is noted that the strongest pressure oscillation occurs in modes II & W.N. and IIs & W.N. (e.g. cases 2 and 3 with the maximum pressure oscillation amplitudes above 750 atm), which correspond to the detonation wave from the hot spot directly hitting the end wall. Besides, modes II and IIs with detonation development from the hot spot (e.g. cases 1, 2, 3, 7 and 8 with the maximum pressure oscillation amplitudes above 200 atm) may cause super-knock while mode W.D. with detonation development from the end wall (e.g. case 5) can hardly produce pressure oscillation strong enough for super-knock. It is noted that one-dimensional case is considered here and the multi-dimensional effects are not included. Therefore there is no Mach stem or triple point which can lead to extreme pressure oscillation near wall. In a real engine, autoignition near the end wall may initiate detonation wave propagating along the wall and cause strong pressure oscillation at adjacent walls. Therefore, as an extension of the present work, it would be interesting to take into account the multi-dimensional effects in future works. It is also emphasized that the correspondence between the autoignition modes from the hot spot (see Fig. 6a) and those near the end wall (see Fig. 6b) is not limited by the cases discussed in this study. The autoignition regimes in ξ-ε and ξ-θ diagrams may quantitatively depend on different factors including the initial temperature and pressure, mixture composition, hot spot (size, temperature gradient), chamber size, and chamber geometry (planar, cylindrical or spherical), which deserves further investigation. Besides, it is expected that the wall reflection effects are similar, at least qualitatively, for different fuels. More realistic fuel models such as PRF and TRF need to be considered in future works.

4. Conclusions

The 1D transient autoignition process initiated by a hot spot in a stoichiometric iso-octane/air mixture inside a small closed chamber is numerically investigated considering detailed chemistry and transport. The effects of shock/pressure wave propagation and reflection on the end wall are systematically investigated. It is found that the autoignition in a small chamber consists of two parts, i.e., (1) the rightwards propagating autoignition front initiated by the hot spot, and (2) the leftwards propagating autoignition front from the end wall induced by the shock/pressure wave reflection. Five autoignition modes from the hot spot are identified and quantitatively described in ξ-ε diagram. Three autoignition modes from the end wall including detonation development are also identified. A new non-dimensional parameter, θ, is introduced to quantify the interplay between different length and time scales. The autoignition modes from the end wall are quantified in ξ-θ diagram. A combination of ξ-ε and ξ-θ diagrams gives a quantitative prediction of autoignition modes caused by a hot spot in a small closed chamber. Besides, it is demonstrated using 1D simulation that detonation developed from the hot spot may cause super-knock while detonation developed from the end wall can hardly produce pressure oscillation strong enough for super-knock. Obviously, the one-dimensional simulation used in the present work cannot account multi-dimensional effects. To clarify this issue further research will be required. Mechanisms of different autoignition modes can be interpreted with the help of ξ-ε and ξ-θ diagrams. Nevertheless, further investigation on the influence of initial conditions and fuels on the autoignition regimes in ξ-ε and ξ-θ diagrams is still needed. Besides, mixture composition effects including stratification [23,25] and fuel-lean and diluted conditions [24] were found to greatly affect the autoignition characteristics. Therefore, further studies for mixtures at different equivalence ratios and dilutions are needed.

Declaration of Competing Interest

The authors declare that they have no known competing financial interests or personal relationships that could have appeared to influence the work reported in this paper.

Acknowledgments

This work is supported by NSFC grants (Nos. 51976088 and 51606091) and Shenzhen Sci-Tech Fund (No. JCYJ20180302173952945).

Supplementary materials

Supplementary material associated with this article can be found, in the online version, at doi:10.1016/j.proci.2020.09.025.

References

[1] Z. Wang, H. Liu, R.D. Reitz, *Prog. Energy Combust. Sci.* 61 (2017) 78–112.
[2] G. Kalghatgi, *Int. J. Engine Res.* 19 (2018) 7–20.
[3] G.T. Kalghatgi, D. Bradley, *Int. J. Engine Res* 13 (2012) 399–414.
[4] Z. Wang, H. Liu, T. Song, et al., *Int. J. Engine Res.* 16 (2015) 166–180.
[5] Z. Wang, Y. Qi, X. He, J. Wang, S. Shuai, C.K. Law, *Fuel* 144 (2015) 222–227.
[6] M. Ohtomo, H. Miyagawa, M. Koike, N. Yokoo, K. Nakata, *SAE Int. J. Fuels Lubr.* 7 (2014) 673–682.
[7] T. Kuboyama, Y. Moriyoshi, K. Morikawa, *SAE Int. J. Engines* 8 (2015) 529–537.
[8] P. Haenel, P. Seyfried, H. Kleeberg, D. Tomazic, Systematic Approach to Analyze and Characterize Pre-Ignition Events in Turbocharged Direct-Injected Gasoline Engines, SAE Technical Paper 2011-01-0343 (2011).
[9] Y.B. Zeldovich, V.B. Librovich, G.M. Makhviladze, G.I. Sivashinsky, *Acta Astronaut.* 15 (1970) 313–321.
[10] Y.B. Zeldovich, *Combust. Flame* 39 (1980) 211–214.
[11] X.J. Gu, D.R. Emerson, D. Bradley, *Combust. Flame* 133 (2003) 63–74.
[12] D. Bradley, C. Morley, X.J. Gu, D.R. Emerson, Amplified Pressure Waves During Autoignition: Relevance to CAI Engines, SAE Technical Paper, 2002-01-2868 (2002).
[13] L. Bates, D. Bradley, G. Paczko, N. Peters, *Combust. Flame* 166 (2016) 80–85.
[14] A. Robert, S. Richard, O. Colin, T. Poinsot, *Combust. Flame* 162 (2015) 2788–2807.
[15] A. Guerouani, A. Robert, J.-M. Zaccardi, Detonation Peninsula for TRF-air Mixtures: Assessment for the Analysis of Auto-Ignition Events in Spark-Ignition Engines, SAE Technical Paper, 2018-01-1721 (2018).
[16] N. Peters, B. Kerschgens, G. Paczko, Super-knock Prediction Using a Refined Theory of Turbulence, SAE Technical Paper, 2013-01-1109 (2013).
[17] C. Wang, C.G. Qian, J.N. Liu, M.A. Liberman, *Combust. Flame* 197 (2018) 400–415.
[18] M.A. Liberman, C. Wang, C.G. Qian, J.N. Liu, *Combust. Theory Model.* 23 (2019) 467–495.
[19] A. Sow, B.J. Lee, F.E.H. Perez, H.G. Im, *Proc. Combust. Inst.* 37 (2019) 3529–3536.
[20] P. Dai, Z. Chen, S.Y. Chen, Y.G. Ju, *Proc. Combust. Inst.* 35 (2015) 3045–3052.
[21] P. Dai, Z. Chen, *Combust. Flame* 162 (2015) 4183–4193.
[22] P. Dai, C.K. Qi, Z. Chen, *Proc. Combust. Inst.* 36 (2017) 3643–3650.
[23] P. Dai, Z. Chen, *Proc. Combust. Inst.* 37 (2019) 4813–4820.
[24] P. Dai, Z. Chen, X.H. Gan, *Combust. Flame* 201 (2019) 208–214.
[25] C.K. Qi, P. Dai, H. Yu, Z. Chen, *Proc. Combust. Inst.* 36 (2017) 3633–3641.
[26] H. Yu, Z. Chen, *Combust. Flame* 162 (2015) 4102–4111.
[27] H. Yu, C.K. Qi, Z. Chen, *Proc. Combust. Inst.* 36 (2017) 3533–3541.
[28] J.Y. Pan, G.Q. Shu, P. Zhao, H.Q. Wei, Z. Chen, *Combust. Flame* 164 (2016) 319–328.

[29] J.Y. Pan, H.Q. Wei, G.Q. Shu, R. Chen, *Combust. Flame* 185 (2017) 63–74.
[30] H. Terashima, M. Koshi, *Combust. Flame* 162 (2015) 1944–1956.
[31] H. Terashima, A. Matsugi, M. Koshi, *Combust. Flame* 203 (2019) 204–216.
[32] H. Wang, M.F. Yao, R.D. Reitz, *Energy Fuels* 27 (2013) 7843–7853.
[33] Z. Chen, M.P. Burke, Y.G. Ju, *Proc. Combust. Inst.* 32 (2009) 1253–1260.